**Proceedings of ASME Turbo Expo 2011**
**GT2011**
**June 6-10, 2011, Vancouver, British Columbia, Canada**

# GT2011-45165

# EXTENSIONS OF CAMPBELL'S MAJOR RESONANCE WITH AN EXPERIMENTAL DEMONSTRATION FOR A COUNTER-ROTATING TURBINE

Robert P. Czachor
Chief Consulting Engineer, Structures
GE Aircraft Engines
1 Neumann Way
Cincinnati, Ohio 45215
PH: (513) 243-2440 FX: (513) 243-1345
EMAIL: ROBERT.CZACHOR@AE.GE.COM

## ABSTRACT

The interaction of vibratory traveling waves in rotating components with adjacent structures is examined. In the most general case, a resonance can occur when the wave propagation speed for a nodal diameter $n$ mode in rotor 1 is equal in speed and direction to the rotational speed of an adjacent structure $\omega_2$. When $\omega_2 = 0$ this structure is a stator and the phenomenon is a major resonance, as discussed in Wilfred Campbell's paper [1] of 1924. An identical phenomena can occur when $\omega_2 \neq 0$ between rotor 1 and a co- or counter-rotating rotor 2 if a suitable harmonic excitation is generated. Description of component test results which demonstrated this resonance mechanism is provided.

## 1. INTRODUCTION- MAJOR RESONANCE IN A ROTOR/ STATOR SYSTEM FOR $n \geq 2$

Campbell [1] investigated certain rim failures of steam turbine wheels, and found that they were caused by a resonant backward-traveling wave in the disk, where the vibration resulted in axial motion of the bladed disk rim and the frequency appeared to be zero relative to a stationary observer. The root cause was shown in what is now commonly known as a Campbell diagram, reproduced here with annotations as Fig. 1. (Fig.1 uses the notation from Ref. [1] which does not appear elsewhere in the present paper)

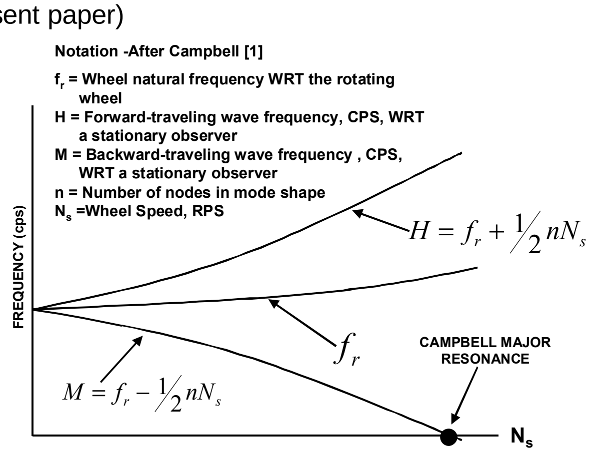


**Figure 1; Campbell Major Resonance From [1]**

It will be the object of this paper to show that the subject of Campbell's investigation was a subset of a more general class of interactions. To better describe this family of vibratory phenomena, a different sign convention will be used. The key definition is that the direction of rotation of the primary rotor, or rotor 1, is taken as positive and that likewise the sign of any traveling wave propagation speed (And corresponding frequency) in the system is also taken as positive if in the same direction as rotor 1 rotation.

The equations for the forward and backward waves in the disk from Fig. 1 can then be expressed as:

$$ {}^n f_{r_1 fwd_g} = {}^n f_{r_1 comb_1} + n\omega_1 \tag{1} $$

$$ {}^n f_{r_1 bkwd_g} = -{}^n f_{r_1 comb_1} + n\omega_1 \tag{2} $$

(Note that frequency terms, $f$, as used throughout this paper, are assumed to include the effects of speed stress-stiffening and temperature per [1], unless otherwise indicated)

In addition, rather than using the equations describing the traveling wave behavior of a disk, the more general form [2] of the equations, which can also describe the traveling wave behavior for a rotating cylinder[1] will be used.

$$ {}^n f_{r_1 fwd\,g} = f_{r_1 comb\,g} + n\omega_1 \left\{ \frac{n^2 - 1 + {}^n\lambda_{r_1}}{n^2 + 1 + {}^n\lambda_{r_1}} \right\} \tag{3} $$

$$ {}^n f_{r_1 bkwd\,g} = -{}^n f_{r_1 comb\,g} + n\omega_1 \left\{ \frac{n^2 - 1 + {}^n\lambda_{r_1}}{n^2 + 1 + {}^n\lambda_{r_1}} \right\} \tag{4} $$

where the $\lambda$ term is a function of the rotor geometry and fixity. For the case of a cylinder fixed at one end, ${}^n\lambda_{r_1}$ is a function of cylinder radius, length, and nodal diameter as given by:

$$ {}^n\lambda_{r_1} = \frac{3R_{r_1}^{\,2}}{n^2 L_{r_1}^{\,2}} \tag{5} $$

[1] As described in Ref. [2] the terms cylinder and disk refer to axisymmetric bodies whose vibratory motion is primarily radial or axial, respectively, rather than to the specific geometry of the component.

 

For a disk, $R/L \to \infty$ and ${}^n\lambda_{r_1} \to \infty$ in Eq. (3) and (4), which results in those equations reducing back to Eq. (1) and (2), respectively. (From a practical standpoint, the difference between disk and cylinder behavior[2] is significant only for lower values of $R/L$ and lower values of $n$ ).

A final modification can be made by casting the diagram in terms of wave propagation speed, rather than frequency, using the relation:

$$\omega WP = f/n \tag{6}$$

For the nodal diameter modes of axisymmetric components under consideration, $\omega WP$ is simply the apparent speed of rotation of the traveling wave. Eq. (3) and (4) then become:

$${}^n\omega WP_{r_{1fwd\,g}} = \frac{{}^n f_{r_{1comb\,g}}}{n} + \omega_1 \left\{ \frac{n^2 - 1 + {}^n\lambda_{r_1}}{n^2 + 1 + {}^n\lambda_{r_1}} \right\} \tag{7}$$

$${}^n\omega WP_{r_{1bkwd\,g}} = -\left( \frac{{}^n f_{r_{1comb\,g}}}{n} \right) + \omega_1 \left\{ \frac{n^2 - 1 + {}^n\lambda_{r_1}}{n^2 + 1 + {}^n\lambda_{r_1}} \right\} \tag{8}$$

The more generalized Campbell diagram which results is shown in Fig. 2.

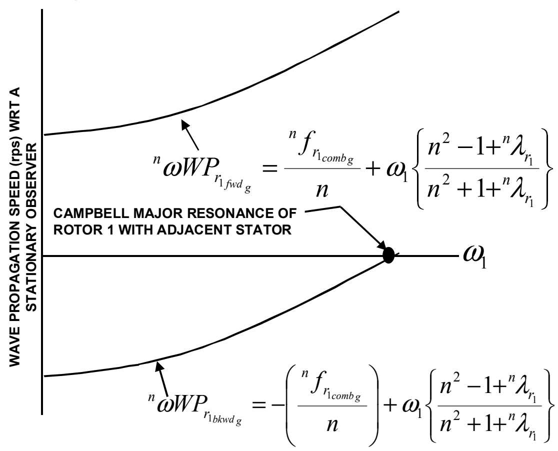


**Figure 2; Campbell [1] Major Resonance in Terms Of Wave Propagation Speed With Revised Sign Convention**

This formulation allows us to define the original Campbell major resonance as when the backward wave propagation speed in rotor 1 is stationary relative to the adjacent structure. The use of wave propagation speed, rather than frequency, allows a direct illustration of the coincidence of component vibratory response with the adjacent rotor speed in the discussions which follow.

## 2. CAMPBELL STATOR RESONANCE FOR $n \geq 2$

A corresponding resonance dependent on a traveling wave in the stator, rather than the rotor, can easily be imagined based on the preceding discussion. If the wave propagation speed in the stator is equal to the speed of an interfacing rotor, a resonant condition, termed a Campbell Stator Resonance by the author, can exist, as shown in Fig. 3.

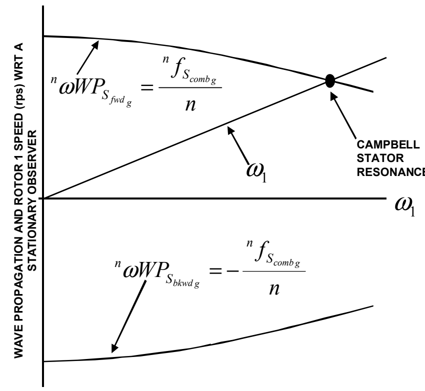


**Figure 3; Campbell Stator Resonance; Wave Propagation Speed WRT Stationary Observer**

The Campbell resonance discussed in Section 1 was characterized by a pattern of equi-spaced rubs on the stator and resulted from vibratory activity in the rotor, dependent on the rotor natural frequency and speed. The Campbell Stator resonance shown in Fig. 3 is governed by the natural frequency of the stator. Excitation of the stator resonance at the proper rotor speed will result in periodic contact on the rotor.

An example of such a resonance, which resulted in a damaging $n = 13$ rub pattern on a rotating seal, was discussed in Ref. [4].

## 3. MAJOR RESONANCE IN COUNTER-ROTATING SYSTEMS FOR $n \geq 2$

The stationary structure discussed in Section 1 may be considered as rotor 2 for the special case of . $\omega_2 = 0$ . The condition of a major resonance in a system of two counter-rotating rotors then becomes apparent as when the wave propagation speed of the backward-traveling wave in rotor 1 is equal to the physical speed of rotor 2, resulting in a resonance of rotor 1, as is shown in Fig. 4.

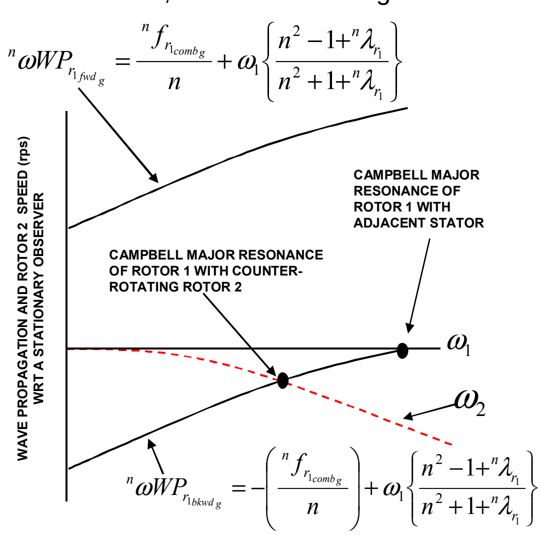


**Figure 4; Campbell Major Resonance in a Counter-Rotating System; Wave Propagation Speed WRT Stationary Observer**

[2] For a free-free cylinder, $\lambda = 0$ , so that the behavior of any geometry can then be bracketed between the limiting possible values of $\lambda$ .

(In the present sign convention, the speed of counter-rotating rotor 2 is a negative number, as is the wave propagation speed of the backward wave in rotor 1)

Conversion of all quantities in Fig. 4 back into the frequency domain returns Eq. (3) and (4) as shown in Fig. 5.

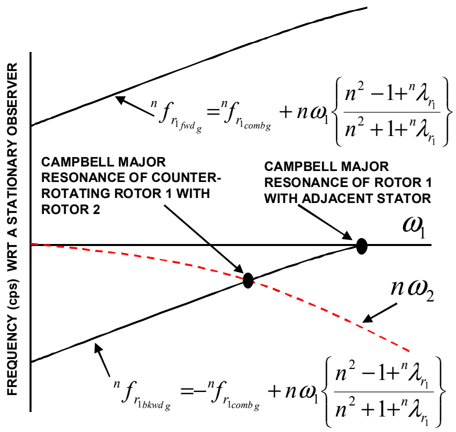


**Figure 5; Campbell Major Resonance in a Counter-Rotating System; Frequency WRT Stationary Observer**

Fig 5. shows that, in order to excite the Campbell major resonance of rotor 1 with a counter-rotating rotor 2, rotor 2 must, by some mechanism, produce an excitation of frequency $n\omega_2$ relative to a stationary reference frame. This mechanism might be an $n\omega_2$ component of frequency in the "white noise" excitation resulting from a rotor/ rotor rub, or as could result from a pattern of rotor 2 dimensional variation with the proper harmonic. Aerodynamic differences among the rotor 2 airfoils might also generate a suitable excitation by means of a resulting harmonic pressure distribution adjacent to rotor 1.

An alternate form of Fig. 5 can be generated by converting that figure to the reference frame of rotor 1 by subtracting $\omega_1$ from Eq. (7) and (8) and then factoring by $n$ to return to the frequency domain:

$$\begin{aligned} {}^{n}f_{r_{1fwd_1}} &= n\left({}^{n}\omega WP_{r_{1fwd_g}} - \omega_1\right) \\ &= n\left(\frac{f_{r_{1comb_g}}}{n} + \omega_1\left\{\frac{n^2-1+{}^{n}\lambda_{r_1}}{n^2+1+{}^{n}\lambda_{r_1}}\right\} - \omega_1\right) \\ &= {}^{n}f_{r_{1comb_g}} - \frac{2n\omega_1}{n^2+1+{}^{n}\lambda_{r_1}} \end{aligned} \tag{9}$$

$$\begin{aligned} {}^{n}f_{r_{1bkwd_1}} &= n\left(-{}^{n}\omega WP_{r_{1bkwd_g}} - \omega_1\right) \\ &= n\left(-\frac{f_{r_{1comb_g}}}{n} + \omega_1\left\{\frac{n^2-1+{}^{n}\lambda_{r_1}}{n^2+1+{}^{n}\lambda_{r_1}}\right\} - \omega_1\right) \\ &= -{}^{n}f_{r_{1comb_g}} - \frac{2n\omega_1}{n^2+1+{}^{n}\lambda_{r_1}} \end{aligned} \tag{10}$$

The excitation from rotor 2 then becomes, in this same reference frame of rotor 1,

$$nf_{\Sigma} = n(\omega_2 - \omega_1) \tag{11}$$

Fig. 6 results and illustrates the signal expected from a rotor 1 strain gage when, for the counter-rotating system, the backward wave in rotor 1 is excited by the proper harmonic of the sum frequency $f_{\Sigma}$ with rotor 2.

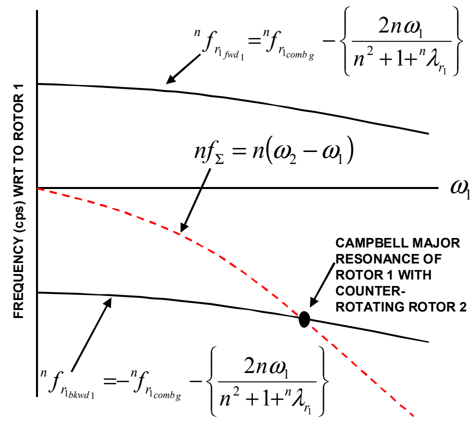


**Figure 6; Campbell Major Resonance in a Counter-Rotating System; Frequency WRT Rotor 1**

The preceding discussion is confined to the prediction of the response of rotor 1; The evaluation for potential resonances of rotor 2 could be conducted in a like fashion by plotting the frequencies of rotor 2 against the speed of rotor 1.

## 4. MAJOR RESONANCE IN CO-ROTATING SYSTEMS FOR $n \geq 2$

A similar phenomena can occur in co-rotating turbomachinery by an identical mechanism. Fig. 7 illustrates the problem in terms of wave propagation speed. The coincidence of rotor 1 wave propagation speed and rotor 2 physical speed again defines the resonance. The plot is similar to that of Fig. 4 except that the resonant crossing now occurs in the upper quadrant where the speed of the forward wave in rotor 1 coincides with the positive speed of co-rotating rotor 2.

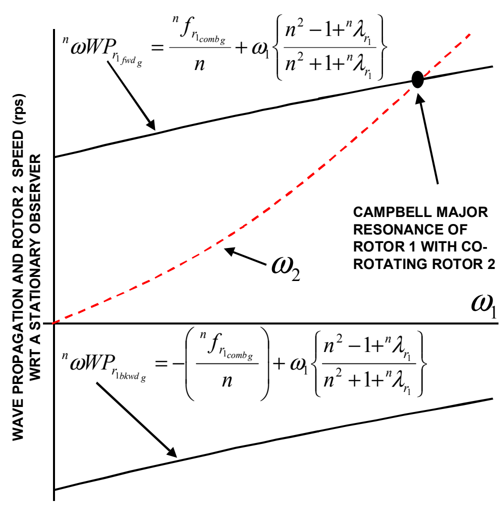


**Figure 7; Campbell Major Resonance in a Co-Rotating System; Wave Propagation Speed WRT a Stationary Observer**

Conversion of the quantities in Fig. 7 to the frequency domain results in Fig. 8. Once again, it is clear that rotor 2 must generate an excitation at the proper harmonic of $\omega_2$ to produce the resonance.

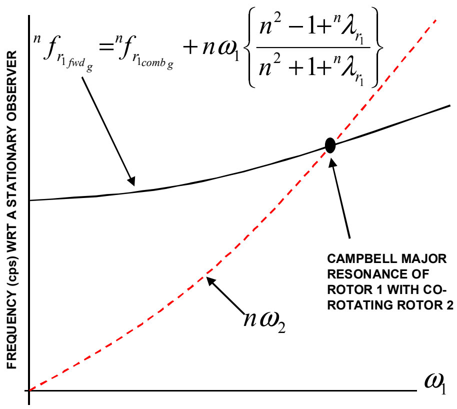


**Figure 8; Campbell Major Resonance in a Co-Rotating System; Frequency WRT A Stationary Observer**

Examination of this same problem from the reference frame of rotor 1 can be accomplished as before resulting in Fig. 9, with $^{n}f_{r_{1fwd_1}}$ described by Eq. (9). The resonance, as indicated by a rotor 1 strain gage, would, in this case, reflect the excitation of the forward wave in rotor 1 by the appropriate harmonic of the difference frequency, $f_\Delta$.

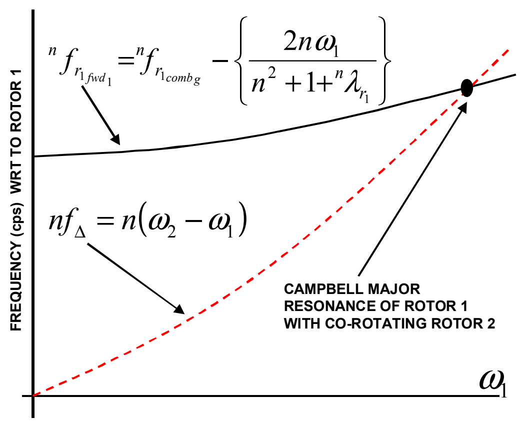


**Figure 9; Campbell Major Resonance in a Co-Rotating System; Frequency WRT Rotor 1**

Unlike the counter-rotating problem, the higher-speed rotor 2 cannot interact in a similar fashion with rotor 1 since, by definition, $\omega_2 > \omega_1$ and therefore:

$$\left\{{}^{n}\omega WP_{r_{2fwd\,g}} = \frac{f_{r_{2comb2}}}{n} + \omega_2\right\} > \omega_1 \tag{12}$$

## 5. MAJOR RESONANCE IN CO- OR COUNTER-ROTATING SYSTEMS FOR $n=1$

The discussion so far has been limited to modes of $n \geq 2$. Similar phenomena in co- and counter-rotating systems[3] where $n=1$, for the so-called “beam bending” modes of the rotors, as also discussed in [5], will now be considered.

[3] Campbell [1] showed that a major resonance in a rotor/ stator system was not possible for an $n=1$ mode.

Relative to the previous discussion, these modes exhibit three unique characteristics:

1. For $n=1$, $\omega WP = f$
2. The asymmetry inherent in the rotor support stiffness of any practical turbomachine results in the generation of both $+\omega_2$ and $-\omega_2$ excitations (Propagating both forward and backward[4] relative to the direction of rotor 2 rotation, as explained in Appendix 1) capable of interacting with the rotor 1 $n=1$ modes.
3. Special mechanisms, such as harmonic dimensional or pressure variation, necessary to generate the $n\omega_2$ excitation required for co- or counter-rotating resonance when $n \geq 2$, are not needed to generate an $n=1$ response. Therefore, such excitations and the resulting resonances are much more likely to be encountered.

The following discussion will utilize the traveling wave equations specific to a disk, rather than the more generalized forms used earlier. This is because the mechanisms (Conservation of momentum and centrifugal forces) which generate the divergence of the forward and backward wave frequencies [2] in cylindrical geometries are not relevant for the $n=1$ modes under discussion.

Fig. 10, then, shows Eq. (1) and (2) converted to wave propagation speed along with the $\pm\omega_2$ excitation lines for a counter-rotating system. (The corresponding plot for co-rotating rotors would be identical with the exception that the $-\omega_2$ locus would lie in the negative quadrant and $+\omega_2$ in the positive)

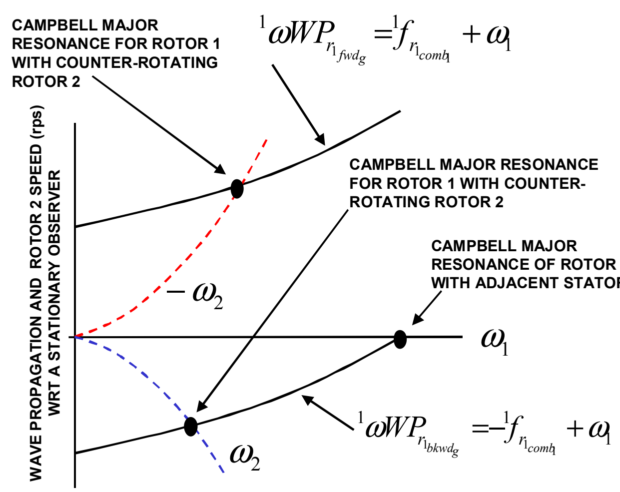


**Figure 10; Campbell Major Resonance in a Counter-Rotating System; Wave Propagation Speed WRT Stationary Observer for $n=1$ Modes**

[4] Higher-order backward-propagating excitations ($-n\omega_2$) have not been observed and therefore were not considered in the previous sections.

When Fig. 10 is converted to the frequency domain in the reference frame of rotor 1, the $\pm\omega_2$ excitations are transformed into the sum ($f_\Sigma$) and difference ($f_\Delta$) frequencies as shown in Fig. 11.

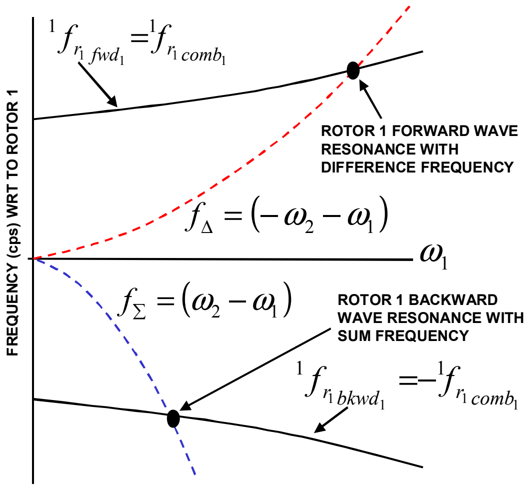


**Figure 11 Campbell Major Resonance in a Counter-Rotating System; Frequency WRT Rotor 1 for $n=1$ Modes**

Fig. 11 illustrates the response of a strain gage on rotor 1 and shows that the backward wave can be excited by the sum frequency and the forward wave by the difference frequency.

Rotor 1 and rotor 2 would each require an evaluation for potential resonance using these techniques. With the present sign convention, the corresponding evaluation for a co-rotating system would result in a plot identical in form to Fig. 11.

Sum and difference excitation of LP turbine rotor $n=1$ modes in response to imbalance in the HP spool is a common observation in co-rotating turbomachinery produced by the author's company.

## 6. EXPERIMENTAL VERIFICATION FOR MAJOR RESONANCE IN A COUNTER-ROTATING SYSTEM

Certain legacy counter-rotating turbines [3] were executed so as to avoid the resonance described in Section 3 by means of suitable frequency placement. However, this constraint can carry a considerable weight penalty. It was therefore determined to validate the preceding calculations by means of a component test designed to demonstrate an $n=2$ resonance in a counter-rotating system. As shown in Fig. 12 and 13, the test set-up simulated an inner turbine stage interfacing with segmented honeycomb shrouds carried by a counter-rotating outer rotor.

The rig was installed in an available facility which was originally designed for the testing of railway braking equipment.

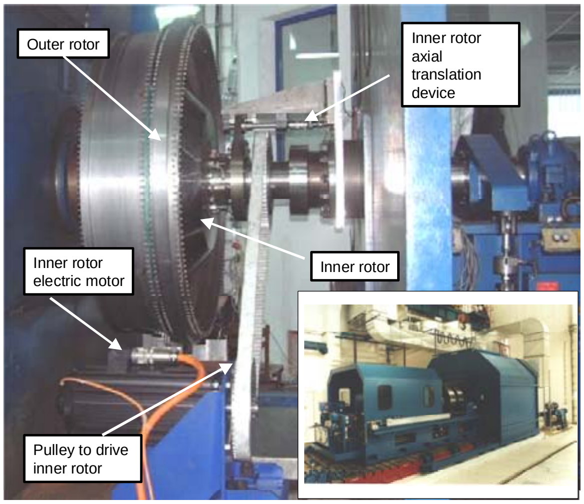


**Figure 12; Counter-Rotating Rotor Rub Test Hardware and Test Facility**

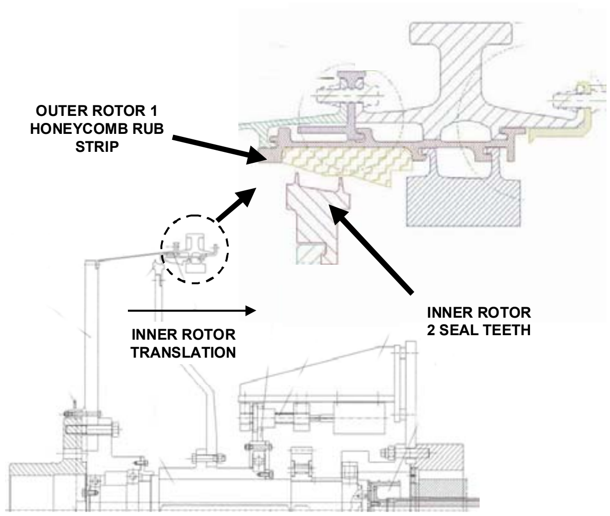


**Figure 13; Counter-Rotating Rub Test Cross-Section Details**

The outer rotor honeycomb shroud segments were designed with a conical inner diameter, such that axial translation of the inner rotor could be used to create a rub of any desired incursion rate and radial depth. The inner rotor seal teeth were machined in an $n=2$ shape, $\pm 0.13$ mm (0.050 in.) on the radius, to ensure the desired excitation.

Designating the outer, T-disk as Rotor 1, the key test parameters were as follows:

$$^2\lambda_{r_1} = 2.6844 \qquad \omega_1 = 36.17 rps \qquad \omega_2 = -30 rps$$

Static and rotating tests of the instrumented outer rotor using a siren as the excitation source were conducted for frequency characterization. For the stationary outer rotor, the $n=2$ mode was identified at 83 cps. Frequencies obtained from the rotating tests for a variety of speeds established the speed stress-stiffening factor as $B=2.66$ by means of Eq. (13) and a curve fit to the frequency vs. speed data. A Fast Fourier Transform of the Rotor 1 frequency data taken at $\omega_1 = 36.17$ rps is shown in Fig. 14 as an example.

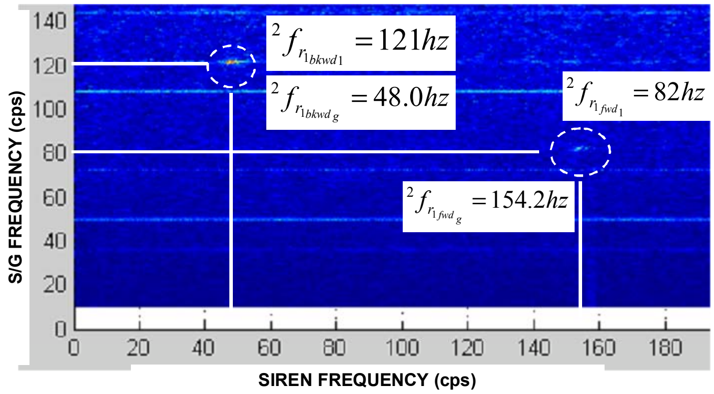


**Figure 14; Counter-Rotating Rub Test Outer Rotor Frequency Data for $\omega_1 = 36.17$ rps**

From the test data, the combined mode frequency at speed can be determined using the well known equation for speed stress-stiffening [1],

$$^2f_{r_{1comb_g}} = \sqrt{\left[{}^2f^{SRT}_{r_{1comb_g}}\right]^2 + \left[B\omega_1^{\,2}\right]} \tag{13}$$
$$= \sqrt{(83)^2 + [2.66(36.17)^2]} = 101.8cps$$

Applying Eq. (9) for the forward wave frequency in the rotating reference frame,

$$^2f_{r_{1fwd_1}} = {}^nf_{r_{1comb_g}} - \frac{2n\omega_1}{n^2 + 1 + {}^n\lambda_{r_1}} \tag{14}$$
$$= 101.8 - \frac{(2)(2)(36.17)}{2^2 + 1 + 2.6844} = 82.97cps$$

which corresponds closely to the observed strain gage signal shown in Fig. 14. Eq. (3) can then be used to obtain the corresponding frequency relative to a stationary observer as follows:

$$^2f_{r_{1fwd\,g}} = {}^nf_{r_{1comb_g}} + n\omega_1\left\{\frac{n^2 - 1 + {}^n\lambda_{r_1}}{n^2 + 1 + {}^n\lambda_{r_1}}\right\} = \tag{15}$$
$$101.8 + (2)(36.17)\left\{\frac{2^2 - 1 + 2.6844}{2^2 + 1 + 2.6844}\right\} = 155.3cps$$

which is nearly equal to the observed siren frequency at resonance with the forward wave of 154.2 cps. For the backward wave, using Eq. (10) to obtain the expected strain gage response:

$$^2f_{r_{1bkwd_1}} = -{}^2f_{r_{1comb_g}} - \frac{2n\omega_1}{n^2 + 1 + {}^n\lambda_{r_1}} \tag{16}$$
$$= -101.8 - \frac{(2)(2)(36.17)}{2^2 + 1 + 2.6844} = -120.63cps$$

which matches well with the measured value of 121 cps (Displayed as a positive number in Fig.14). Finally, Eq. (4) can be used to convert this result to the stationary reference frame:

$$^2f_{r_{1bkwd\,g}} = -{}^nf_{r_{1comb_g}} + n\omega_1\left\{\frac{n^2 - 1 + {}^n\lambda_{r_1}}{n^2 + 1 + {}^n\lambda_{r_1}}\right\} = \tag{17}$$
$$-101.8 + (2)(36.17)\left\{\frac{2^2 - 1 + 2.6844}{2^2 + 1 + 2.6844}\right\} = -48.29cps$$

a result also in good agreement with the test siren frequency (Again displayed as a positive number in Fig. 14) of 48 cps.

Campbell diagrams similar to those presented previously can now be constructed. In this test, the outer rotor speed $\omega_1$ was held constant, so a diagram similar to Fig. 4 can be constructed except with $\omega_2$ as the positive X-axis. Values for the rotor 1 wave propagation speeds can be calculated from the results of Eq. (16) and (17) using Eq. (6) with the corresponding Campbell diagram shown as Fig. 15.

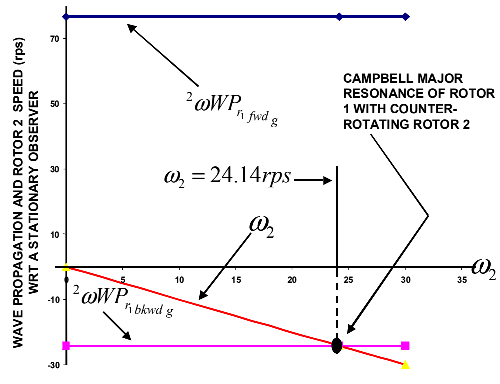


**Figure 15; Rub Test Campbell Diagram; Wave Propagation Speed WRT Stationary Observer**

An $n = 2$ resonance would therefore be expected at an inner rotor speed of 24.14 rps. Conversion of Fig. 15 into the frequency domain and reference frame of rotor 1 yields Fig.16.

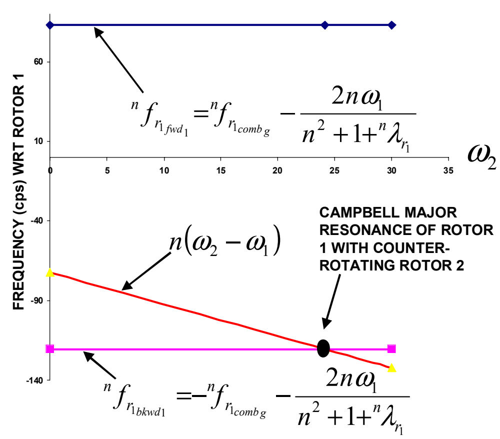


**Figure 16; Rub Test Campbell Diagram; Frequency WRT Rotor 1**

Data from a rotor 1 strain gage, taken during the rotor 1/ rotor 2 rub, is shown in Fig. 17. Rotor 1 was maintained at 36.17 rps while rotor 2 was allowed to decelerate from 30 rps as it was translated into the honeycomb and the rub event progressed. The data reduction software which was used plots all quantities of Fig. 16 in the positive quadrant, but the results shown in Fig. 17 are otherwise nearly identical.

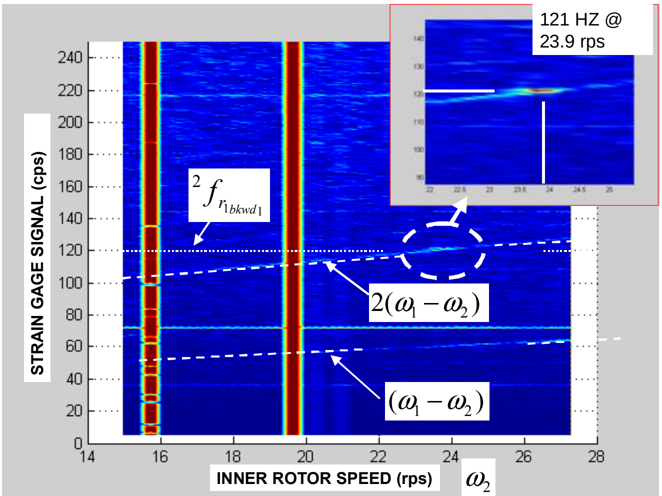


**Figure 17; Rub Test Outer Rotor Frequency Response From Rotor 1/ Rotor 2 Rub Event**

## 7. CONCLUSIONS

A family of Campbell resonance phenomena are characterized by an interaction of a traveling wave for an $n$ diameter mode where the wave propagation speed and direction matches the physical rotational speed of an interfacing structure.

1. When ${}^{n}\omega WP_{r_1}=\omega_2=0$, the wave is stationary in space and a Campbell major resonance as described in Ref. [1] can occur.
2. When ${}^{n}\omega WP_{s}=\omega_2$, a Campbell stator resonance may result as in the example discussed in Ref. [4].
3. When ${}^{n}\omega WP_{r_1}=\omega_2, \omega_2\neq 0$, and $n\geq 2$, a Campbell resonance with a co- or counter-rotating rotor 2 can occur, but only when rotor 2 produces an excitation at the proper harmonic of speed.
4. When ${}^{n}\omega WP_{r_1}=\pm\omega_2$ and $n=1$, the beam-bending modes of rotor 1 can be excited by the sum and difference frequency of the co- or counter-rotating rotors, as observed in the reference frame of rotor 1.

## 8. ACKNOWLEDGEMENTS


The author would like to acknowledge to the work of RA Kirkpatrick and PH Stoughton of GE relative to the problem of Campbell's criteria relative to counter-rotating turbomachinery, as originally encountered on the GE36 UDF™ [3] program. The rig test described in the present work was designed by the GE Engineering Design Center (EDC) in Warsaw, Poland, and tested at the Railway Scientific and Technical Centre (CNTK) facility. Thanks are due to Robert Jamiolkowski and Janusz Maliszewski of EDC, and Joe Albers at GEAE for their contributions to that test and their assistance in the preparation of this paper.


## 9. NOMENCLATURE

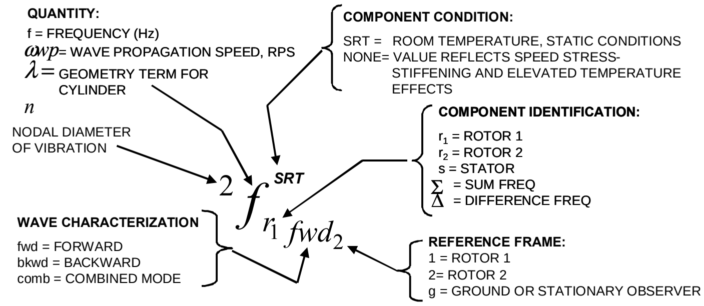


**Figure 18; Nomenclature For Parameter Identification**

$\omega_1$ = Rotor 1 speed in rps; $\omega_1$ defined as $>0$

$\omega_2$ = Rotor 2 speed in rps; $\omega_2$ is a negative number if the direction of rotor 2 rotation is opposite rotor 1. For co-rotating systems $\omega_2>0$ and is defined as the higher speed rotor. ($\omega_2>\omega_1$)

$B$ = Speed stress-stiffening frequency correction factor

Backward-Traveling Wave = A traveling wave where the direction of wave propagation is in the direction opposite to the rotation of the vibrating rotor. $f_{bkwd}<0$ if the direction of wave propagation is opposite to rotor 1 rotation.

Combined Mode = A mode shape consisting of the superposition of the forward and backward waves. This is the vibratory mode as measured in a frequency test of a stationary axisymmetric component where fixed nodes and anti-nodes are observed. $f_{comb}$ is defined as positive.

Forward-Traveling Wave = A traveling wave where the direction of wave propagation is in the same direction as the rotor rotation. $f_{fwd}>0$ if the direction of wave propagation is the same as rotor 1 rotation.

$f$ = Frequency in cps. $f$ has the same sign as the corresponding $\omega WP$ and is assumed to include the effects of speed stress-stiffening and temperature as appropriate unless modified by a superscript ($f^{SRT}$) indicating a value reflecting room-temperature, static conditions.

$f_{\Sigma}$ **=** Sum frequency, $\pm(\omega_1+|\omega_2|)$ , cps

$f_{\Delta}$ **=** Difference frequency, $\pm(\omega_1-|\omega_2|)$, cps

**L** = Length of an axisymmetric component

$\lambda$ = Geometry term for an axisymmetric component

$n$ = Number of nodal diameters (Complete waves) in the vibratory mode shape of an axisymmetric structure, whose deflection can be described as $\delta(\theta)=x\cos n\theta$. Also equal to ½ the number of nodes in the mode shape.

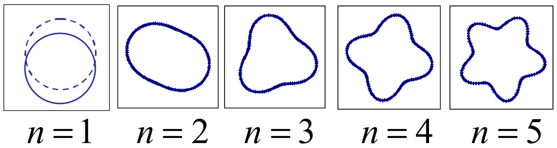


**Figure 19; Example Mode Shapes for Various Nodal Diameters (The plots can be interpreted as either axial or radial deflection, dependent on the vibratory characteristics of the component)**

R = Mean radius of an axisymmetric component

Wave Propagation Speed **=** The apparent speed of rotation in rps of a traveling wave or $\omega WP = f/n$. $\omega WP$ is positive if the wave propagation direction is the same as rotor 1 rotation $\omega_1$.

WRT **=** **W**ith **R**espect **T**o (Reference Frame)

## 10. REFERENCES

[1] Campbell, W., 1924, "The Protection of Steam Turbine Disc Wheels from Axial Vibrations", Trans ASME Vol. 46

[2] Macke, H.J., 11/11/65, "Traveling-Wave Vibration of Gas-Turbine Engine Shells", ASME P65 WA/ GTP-3

[3] GE Aircraft Engines, GE36 Project Dept, 12/87, "Full Scale Technology Demonstration Of A Modern Counter-Rotating Unducted Fan Engine- Design Report", NASA CR 180867, NASA Lewis Research Center NAS 3-24210 (Pages 105-116)

[4] Alford, J.S., 7/2/62, "Protection of Labyrinth Seals from Flexural Vibration", ASME 63-AHGT-9

[5] Anegawa, N., Fujiwara, H., and Matsushita, O., 10/26/10, "Vibration Diagnosis Featuring Blade-Shaft Coupling Effect of Turbine Rotor Models", Journal of Engineering for Gas Turbines and Power, Vol. No. 2

## 11. APPENDIX I; GENERATION OF $\pm\omega$ EXCITATION BY AN UNBALANCED ROTOR WITH ASYMMETRIC SUPPORT STIFFNESS

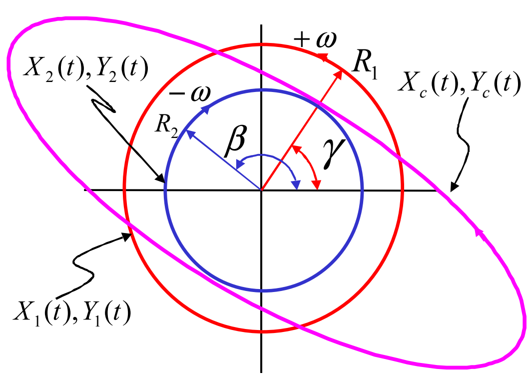


**Figure 20; Components Of Elliptical Unbalanced Motion**

Consider two exactly counter-rotating ($\pm\omega$) circular orbits at $R_1$ and $R_2$ as shown in Fig. 20. These may be considered as the orbits of two unbalanced masses, producing both $\pm\omega$ excitations relative to a stationary observer.

In Cartesian coordinates as a function of time, t, the two motions can be described as

$$X_1(t) = R_1 \sin(\omega t + \gamma) \qquad Y_1(t) = R_1 \cos(\omega t + \gamma)$$
$$X_2(t) = R_2 \sin(-\omega t + \beta) \quad Y_2(t) = R_2 \cos(-\omega t + \beta) \tag{18}$$

where the phase angles $\gamma$ and $\beta$ are arbitrary but unequal, as are $R_1$ and $R_2$.

If now we consider these two orbits as components of a combined motion, the resulting behavior can be obtained by superposition.

Summation of the X coordinates yields:

$$\begin{aligned}
X_c(t) &= R_1 \sin(\omega t + \gamma) + R_2 \sin(-\omega t + \beta) \\
&= R_1 \sin\omega t \cos\gamma + R_1 \cos\omega t \sin\gamma + \\
&\quad R_2 \sin(-\omega t)\cos\beta + R_2 \cos(-\omega t)\sin\beta \\
&= R_1 \sin\omega t \cos\gamma + R_1 \cos\omega t \sin\gamma - \\
&\quad R_2 \sin\omega t \cos\beta + R_2 \cos\omega t \sin\beta \\
&= \{R_1 \cos\gamma - R_2 \cos\beta\}\sin\omega t + \\
&\quad \{R_1 \sin\gamma + R_2 \sin\beta\}\cos\omega t
\end{aligned} \tag{19}$$

Likewise, the summation of coordinates in the Y direction results in:

$$\begin{aligned}
Y_c(t) &= R_1 \cos(\omega t + \gamma) + R_2 \cos(-\omega t + \beta) \\
&= R_1 \cos\omega t \cos\gamma - R_1 \sin\omega t \sin\gamma + \\
&\quad R_2 \cos(-\omega t)\cos\beta - R_2 \sin(-\omega t)\sin\beta \\
&= R_1 \cos\omega t \cos\gamma - R_1 \sin\omega t \sin\gamma + \\
&\quad R_2 \cos\omega t \cos\beta + R_2 \sin\omega t \sin\beta \\
&= \{-R_1 \sin\gamma + R_2 \sin\beta\}\sin\omega t + \\
&\quad \{R_1 \cos\gamma + R_2 \cos\beta\}\cos\omega t
\end{aligned} \tag{20}$$

Assigning new variables to the gathered constants results in the following simplified expressions:

$$X_c(t) = A\sin\omega t + B\cos\omega t$$
$$Y_c(t) = C\sin\omega t + D\cos\omega t \tag{21}$$

Eq. (21) describe elliptical motion in a Cartesian system. A Fourier breakdown of the elliptical displacement path of an unbalanced rotor rotating at speed $\omega$ with an asymmetric support would therefore reveal the $\pm\omega$ frequencies of the circular component motions.